STEM CELLS TRANSLATIONAL MEDICINE®

TISSUE-SPECIFIC PROGENITOR AND STEM CELLS

Human Mesenchymal Stem Cell Grafts Enhance Normal and Impaired Wound Healing by Recruiting Existing Endogenous Tissue Stem/Progenitor Cells

LAURA SHIN, DANIEL A. PETERSON

Key Words. Adult human bone marrow • Mesenchymal stem cells • Stem cell • Cellular therapy • Diabetes • Progenitor cells • Tissue regeneration

Center for Stem Cell and Regenerative Medicine and Department of Neuroscience, Rosalind Franklin University of Medicine and Science, North Chicago, Illinois, USA

Correspondence: Daniel A. Peterson, Ph.D., Department of Neuroscience, Chicago Medical School, Rosalind Franklin University of Medicine and Science, 3333 Green Bay Road, North Chicago, Illinois 60064, USA. Telephone: 847-578-3411; Fax: 847-578-8545; E-Mail: Daniel.Peterson@rosalindfranklin.edu

Received April 17, 2012; accepted for publication October 16, 2012; first published online in SCTM *EXPRESS* December 21, 2012.

1066-5099/2012/$20.00/0

http://dx.doi.org/10.5966/sctm.2012-0041

ABSTRACT

Mesenchymal stem cells (MSCs) have been investigated as a clinical therapy to promote tissue repair. However, the disappearance of grafted cells soon after engraftment suggests a possible role as initiators of repair rather than effectors. We evaluated the relative contribution of grafted human MSCs and host stem/progenitor cells in promoting wound healing by using a novel asymmetric wound model in normal and impaired healing diabetic (*db/db*) mice to discriminate between the effect of direct engraftment and the subsequent systemic response. Experimental animals received paired wounds, with one wound receiving human mesenchymal stem cells (hMSCs) and the other wound receiving vehicle to assess local and systemic effects, respectively. Control animals received vehicle in both wounds. Grafted hMSCs significantly improved healing in both normal and impaired healing animals; produced significant elevation of signals such as Wnt3a, vascular endothelial growth factor, and platelet-derived growth factor receptor-α; and increased the number of pre-existing host MSCs recruited to the wound bed. Improvement was also seen in both the grafted and nongrafted sides, suggesting a systemic response to hMSC engraftment. Healing was enhanced despite the rapid loss of hMSCs, suggesting that mobilizing the host response is the major outcome of grafting MSCs to tissue repair. We validate that hMSCs evoke a host response that is clinically relevant, and we suggest that therapeutic efforts should focus on maximizing the mobilization of host MSCs. STEM CELLS TRANSLATIONAL MEDICINE *2013;2:33–42*

INTRODUCTION

Mesenchymal stem cells (MSCs), a heterogeneous multipotent stromal mesenchymal cell, contribute to tissue maintenance throughout the body [1, 2]. MSCs are attractive for cell-mediated therapies, as they can be grown exponentially and maintain differentiation potential into osteoblasts, chondrocytes, and adipocytes both in vivo and in vitro [3, 4]. Initially it was thought that MSCs effected repair through direct participation in the repair process and eventual incorporation into regenerated tissue [5, 6]. However, this interpretation has been re-examined because of the lack of evidence for MSC assimilation and the disappearance of grafted cells after systemic delivery [7, 8]. It has been difficult to resolve the fate of grafted MSC in studies using systemic delivery because of the short half-life of engrafted MSCs, lack of sensitive means for isolation and detection, and low targeting efficiency [7]. It has been proposed that grafted MSCs modulate the host environment through indirect mechanisms, leading to enhanced healing, rather than through direct participation and incorporation into tissue [9–11]. For example, in patients with bone defects, implanted MSCs may have initiated repair, but the recipients' own osteoprogenitor cells eventually created the new bone [12]. The responsiveness of the grafted MSCs to the host environment is also illustrated by the variable and inconsistent outcomes of clinical trials for diseases such as graft-versus-host disease [13, 14]. In contrast to the direct engraftment and function of transplanted hematopoietic stem cells, MSCs seem to act indirectly in the repair process [10, 15, 16]. Therefore, engrafted MSCs may initiate or facilitate the host repair response and thus act as a vector to deliver the therapeutic signal [12].

Despite the apparent indirect effect of grafted MSCs, the relative contribution of grafted and endogenous stem/progenitor cells to healing is largely unknown [4, 8]. Recently, we have shown that the regenerative capacity of MSCs is impaired in chronic disease states, contributing to poor healing [17]. Endogenous MSC behavior after exiting the bone marrow is unclear, and the regenerative capacity of MSCs appears minimal without exogenous engraftment or stimulation [7]. Furthermore, it is also unknown whether the host responds by recruiting

existing cells or generating new cells in response to MSC delivery. Allogeneic engraftment of mouse MSCs has shown improvement in wound closure, but it is difficult to delineate the contributions of the host and the exogenous cells [17, 18]. The importance of host cells to this process is supported by reduced healing in diabetic mice, whose endogenous MSCs are impaired [17]. We developed an innovative asymmetric wound model and directly engrafted human mesenchymal stem cells (hMSCs) to discriminate the relative contribution of the grafted MSC from the endogenous response in creating a healing environmental niche in an easily accessible wound bed. The immune suppressive characteristics of hMSCs allowed us to use human cells. The use of human cells provided multiple tools for lineage tracing and enabled us to discriminate grafted cells from host cells [7, 19]. We labeled hMSCs with green fluorescence protein (GFP) and used species-specific markers to track and determine the fate of these cells in vivo. We engrafted these cells into paired wounds in wild-type and slow-healing diabetic mice to analyze the host response to MSC engraftment in a normal and impaired healing environment. Experimental animals received paired wounds, with one wound receiving hMSCs and the other wound receiving vehicle to assess local and systemic effects, respectively. Control animals received vehicle in both wounds and served as a naïve/phosphate-buffered saline (PBS) control. We then assessed the differences in healing, signaling, and cell populations over time between the grafted, nongrafted, and naïve/PBS wounds. We also used dual halogenated thymidine analogs to birthdate proliferating cells at distinct times to see whether host cells responding to the hMSC engraftment existed prior to grafting or were generated in response [20].

Here we report that MSCs initiate the formation of a niche in the injured environment and promote recruitment through expressing signals that direct endogenous stem/progenitor cells to the site of injury. We observed (a) the rapid disappearance of engrafted cells and a corresponding increase in the number of host cells to the area of injury in both the impaired and normal healing model, (b) the modulation and recruitment of host cells both locally and systemically in response to exogenous MSC engraftment, (c) the active participation and mobilization of an existing population of endogenous cells in healing with minimal generation of new cells, and (d) an upregulation of gene expression levels of angiogenic and recruitment signals in the wound beds of grafted animals. Grafted cells did not remain in the wound, nor did they translocate to other regions throughout the body, suggesting that their role is largely limited to signaling that initiates the recruitment and direction of endogenous cells.

Materials and Methods

Animal Work

Animals used in this study were obtained from The Jackson Laboratory (Bar Harbor, ME, http://www.jax.org) and consisted of 8-week-old, impaired healing BKS.Cg-*Dock7*^{m}+/+*Lepr*^{db}/J (*db/db*) mice selected from a spontaneous diabetes mutation in the leptin receptor gene (*Lepr*^{db}) and normal healing age-matched nondiabetic heterozygous littermates from a C57BLKS wild-type (WT) background. The *db/db* animals expressed diabetic phenotypes, such as hyperglycemia and obesity, and had impaired wound-healing abilities.

The mice were equilibrated to the animal facility prior to any surgical procedures in cages of five and were housed individually postwounding. Their weights and plasma glucose levels were recorded weekly on the nonwounded animals from nicked tail vein blood at 9:00 a.m. Central Standard Time using an Accu-Chek glucose meter (Roche Diagnostics, Basel, Switzerland, http://www.accu-chek.com). The weights and plasma glucose levels of the designated wounded animals were recorded immediately postwounding and at closure. All animal experiments and procedures have been reviewed and approved by the Rosalind Franklin University of Medicine and Science Institutional Animal Care and Use Committee.

Human Mesenchymal Stem Cell and Mouse Fibroblasts

Human mesenchymal stem cells (hMSCs) were extracted from the bone marrow of the iliac crest of healthy donors. These cells were acquired from the Tulane University Center for Gene Therapy and arrived frozen at passage 1 in 5% dimethyl sulfoxide (DMSO)-complete culture media (CCM: α-minimal essential media, 20% fetal bovine serum, L-glutamine, and penicillin/streptomycin). Cells were plated in CCM at a density of 10,500 cells per 175-cm^2 flask and kept at 37°C in 5% CO_2. The media were changed every 3 days. When cells reached 80% confluence, they were dissociated with trypsin and EDTA. Dissociated cells were then replated in new flasks at the same density during each subsequent passage or frozen down in 5% DMSO in CCM. Fibroblasts from the tail tips of 8-week-old nondiabetic WT mice were derived in-house using CCM.

For lineage tracing post-engraftment, a population of hMSCs was genetically modified to stably express GFP. At passage 3, hMSCs were plated at 250 cells per well on a 12-well plate for cytomegalovirus-GFP lentivirus infection (self-inactivating; gift from Dr. Robert Marr). The optimal vector concentration of 2.59×10^2 transduction units/ml was determined by a serial dilution, and GFP signal was measured using an LSR II flow cytometer (BD Biosciences, San Diego, CA, http://www.bdbiosciences.com). Following validation by flow cytometry, this population was expanded and frozen down to provide stock for the described experiments in this project. In preparation for grafting, labeled cells (passage 2) were isolated by fluorescence-activated cell sorting at $\geq$95% purity for GFP expression. GFP signaling was monitored with flow cytometry analysis after every passage. Cell phenotypes were confirmed by flow cytometric analysis to ensure that the population was positive for CD29 (β-1 integrin; Abcam, Cambridge, MA, http://www.abcam.com), CD44 (Indian blood group; Abcam), CD90 (cell surface glycoprotein marker Thy1; Invitrogen, Carlsbad, CA, http://www.invitrogen.com), and CD166 (activated leukocyte cell adhesion molecule [ALCAM]; BioLegend, San Diego, CA, http://www.biolegend.com) and negative for CD45 (leukocyte common antigen; Abcam), CD34 (hematopoietic progenitor cell antigen; Invitrogen), and CD14 (lipopolysaccharide receptor; R&D Systems Inc., Minneapolis, MN, http://www.rndsystems.com). Cells at $\leq$80% confluence were prepared for grafting to wound beds by dissociation, washing, and resuspension of 1×10^5 cells in 60 μl of PBS for engraftment to each wound bed. Differentiation and colony-forming unit assays were performed on all MSC populations used in this study in accordance with the guidelines proposed by the MSC Committee of the International Society for Cellular Therapy [11].

Excisional Splint Wound Model

We used an established excisional wound splinting technique to closely approximate the human healing model by allowing re-epithelialization and granulation rather than contraction (the normal repair process in rodents) [21]. Allowing granulation tissue formation enabled us to monitor increases in tissue proliferation and organization throughout healing [22]. Eight-week-old *db/db* and age-matched nondiabetic WT normal healing animals were treated with four 15 μl injections of GFP-labeled human MSCs in PBS (1×10^5 cells in total), or four 15 μl injections of PBS only.

Our preliminary studies have shown that immunosuppressive therapies were not necessary with human MSC engraftment (data not shown). Mice were anesthetized with ketamine/xylazine (200 mg/kg and 10 mg/kg) and the dorsal skin was shaved, depilatated, and sterilized with ethanol. Two full-thickness wounds were created using an 8-mm Miltex dermal punch (Integra Miltex, York, PA, http://miltex.com) on the midback of all animals. A donut-shaped silicone splint was centered over the wound and adhered with adhesive glue and simple interrupted sutures. Wounds received four (15-μl) intradermal injections of 100,000 GFP-labeled hMSCs in 60 μl of PBS or four 15 μl injections of PBS using a Hamilton syringe. Placements of the injections were monitored using an Olympus SZX12 stereomicroscope (Olympus, Tokyo, Japan, http://www.olympus-global.com) equipped with excitation/emission filters for GFP. Wounds were covered with Tegaderm dressing (3M, Minneapolis, MN, http://www.3m.com), and animals were housed individually. Wound closure was monitored and documented daily by stereomicroscopy. The surgical dressing was removed and reapplied before and after each measurement. Animals were terminally anesthetized, and wound beds were harvested and dissociated at various time points for histology, flow cytometry, and gene expression analysis. Halogenated thymidine analogs were used to birthdate cell populations as we have described previously [20, 23]. Animals appropriated for proliferation studies received an intraperitoneal injection of a nonradioactive thymidine analog, including iododeoxyuridine (IdU) and/or chlorodeoxyuridine (CldU; 50 mg/kg or equimolar equivalents in sterile saline; up to six injections). A cohort of 10 *db/db* mice and 10 wild-type mice received the bilateral wounds with unilateral engraftment, and another 10 *db/db* and 10 wild-type mice received bilateral wound with vehicle delivery (PBS only) for each time point in this study.

Microscopy and Histology

Wound beds were monitored daily by macroscopic examination using an Olympus SZX12 stereomicroscope equipped with excitation/emission filters for GFP. Digital images were acquired at fixed zoom settings and calibrated against a stage micrometer. Images of each wound bed were taken daily under white light and fluorescent illumination. Wound closure was quantified using the Cavalieri point probe estimator (StereoInvestigator software; MBF Bioscience, Williston, VT, http://www.mbfbioscience.com) to accurately account for irregular and discontinuous profiles of healing tissue within the wound bed.

Gene Expression Analysis

Total RNA Isolation and Reverse Transcription

Quantification of gene expression was used to investigate the role of environmental or MSC cell-autonomous factors expressed within the wound bed during wound healing. Tissue biopsies were used to assess overall environmental expression.

Total RNA from tissue biopsies was extracted using the RNeasy Fibrous Tissue kit (Qiagen, Hilden, Germany, http://www.qiagen.com). This involves sample lysis and homogenization using sterile hard tissue omni probes (Omni International, Kennesaw, GA, http://www.omni-inc.com), followed by a proteinase-K digestion to remove the high number of proteins from connective tissue, contractile fibers, and collagen found in fibrous tissue. The sample was treated with ethanol and applied to an RNeasy spin column. RNA was treated with DNase to remove residual DNA and washed. Purified total RNA was eluted in 60 μl of RNase-free water. Purified RNA was then placed in a speed vacuum to increase RNA concentration.

The resulting purified total RNA was analyzed for quantity and quality by taking only 1 μl of the elution volume for analysis using the RNA 6000 Pico RNA LabChip kit for the Agilent 2100 Bioanalyzer (Agilent Technologies, Palo Alto, CA, http://www.agilent.com). This analysis provided immediate information on the amount of ribosomal and mRNA in addition to the extent of degradation.

Known starting amounts of the isolated total RNA were used for reverse transcription (RT) reactions using the Promega Improm-II Reverse Transcription System (Promega, Madison, WI, http://www.promega.com). This system provided templates for first-strand cDNA synthesis of total RNA using or oligo$(dT)_{15}$ primers (tissue biopsy RNA). Each reaction yielded 20 μl of synthesized cDNA. All reactions were conducted in the presence of the manufacturer's RNase inhibitor.

Quantitative Real-Time Polymerase Chain Reaction

Quantification of target genes was performed from known amounts of generated cDNA using a Bio-Rad iCycler Real-Time PCR System (Bio-Rad, Hercules, CA, http://www.bio-rad.com). We used Bio-Rad SYBR Green supermix containing nucleotides, $MgCl_2$, Taq polymerase, fluorescein, and SYBR Green. The cDNA was added to supermix solution, forward and reverse primers, and RNase-free water to a volume of 25 μl per well in a 96-well plate. A 1:5 standard curve was run with all experimental samples, and all samples were run in triplicate. The standard cDNA was produced in-house from human or mouse MSCs generated from cell culture. A melt curve to check for SYBR Green specificity was included. Negative controls included a sample collection negative control, no-RT-negative control, and no-template control. Human and mouse-specific primers were designed in-house using Beacon Designer software (Premier Biosoft, Palo Alto, CA, http://www.premierbiosoft.com/) and synthesized by Operon (Eurofinns MWG Operon, Huntsville, AL, http://www.operon.com). We implemented mouse primers *Wnt3a* forward (5′-TTCCTGAGCGAGCCTGGGCT-3′), vascular endothelial growth factor-a (*VEGFa*) forward (5′-CAGCCTTCAGCTCGCTCCT-3′), and platelet-derived growth factor receptor-α (*PDGFR*α) forward (5′-AGAGGTCCAGGTGAGGTTAGAGG-3′). Primer amplicons were designed to be $<$100 bp for use with samples. Results were analyzed in comparison with two or more housekeeping genes (GAPDH or β-actin) validated to have lowest intersample variance.

Flow Cytometry

Wound bed tissue was dissociated into a single-cell suspension with trituration and digestion buffer. Minced tissue was placed in

0.25% trypsin/EDTA overnight at 37°C and filtered through a 70-μm nylon cell strainer. Tissue dissociation protocols were adapted for other tissue types included in the project. Cells were then spun down and washed with PBS. For the detection of endogenous MSCs, dissociated cells were incubated with the positive MSC markers CD29 (β-1 integrin; Abcam), CD44 (Indian blood group; Abcam), CD90 (cell surface glycoprotein marker Thy1; Invitrogen), and CD166 (ALCAM; BioLegend). Other non-MSC populations and endothelial progenitor cells were identified using the hematopoietic lineage markers CD45 (LCA; Abcam), CD34 (hematopoietic progenitor cell antigen; Invitrogen), and CD14 (lipopolysaccharide receptor; R&D Systems). All conjugated pairs were incubated at room temperature for 45 minutes. Ten thousand events were analyzed for GFP, allophycocyanin, and phycoerythrin and colabeling using the LSR II flow cytometer with FACSDiva software (BD Biosciences).

Statistical Analysis of Quantitative Data

Between-group data comparisons were made using analysis of variance followed by a Bonferroni post hoc test using the statistical software Prism (GraphPad Software, Inc., San Diego, CA, http://www.graphpad.com). Significance was accepted when $p < .05$. Variance estimates encountered in generating the preliminary data revealed that most forms of analysis required a minimum sample size of 10 subjects per group.

Results

hMSC Grafts Promote Healing of Both Local and Distant Wounds

Paired excisional splint wounds were prepared on the dorsum of either 8-week-old *db/db* or age-matched WT male mice. We chose the *db/db* animal, a well-described model of impaired healing, to evaluate the host response to engraftment and to compare to the host response of WT animals in normal physiologic healing [17]. Control animals received identical paired wounds without hMSC engraftment to measure baseline healing (naïve/PBS; Fig. 1A, 1B). Asymmetrical engraftment with GFP-expressing hMSCs (Fig. 1C, right, hMSC-grafted [G-hMSC] condition) and PBS-only vehicle (Fig. 1C, left, PBS-grafted [G-PBS] condition) helped discriminate between the effect of local delivery of cells and the subsequent systemic response. The response on the grafted side revealed the direct, cell-mediated effect of engraftment, whereas the response on the nongrafted side revealed the extent of the indirect or systemic effect of MSC engraftment on promoting wound healing.

Prior to engraftment, GFP-expressing hMSCs were expanded in culture and prepared for grafting as described. We have validated that GFP-labeled hMSCs are multipotent and express appropriate markers (supplemental online Fig. 1). We also determined hMSCs stably express GFP over time and differentiation. An analysis of healing was made at the following times postgrafting: 1, 5, 10, and 15 days. At each time point, wound beds were biopsied and the tissue allocated for flow cytometric, histological, and molecular analysis (Fig. 1D). Monitoring by macroscopic fluorescence and bright-field observation allowed us to visualize the location of the cells during engraftment and over time (Fig. 1E). GFP-labeled hMSCs could also be detected microscopically (supplemental online Fig. 1A–1J). Abundant GFP-positive hMSCs were observed 1 day following grafting, but their number was sharply reduced by day 5 (supplemental online Fig. 1), and GFP-positive cells were undetectable within the wound bed by day 10 (data not shown).

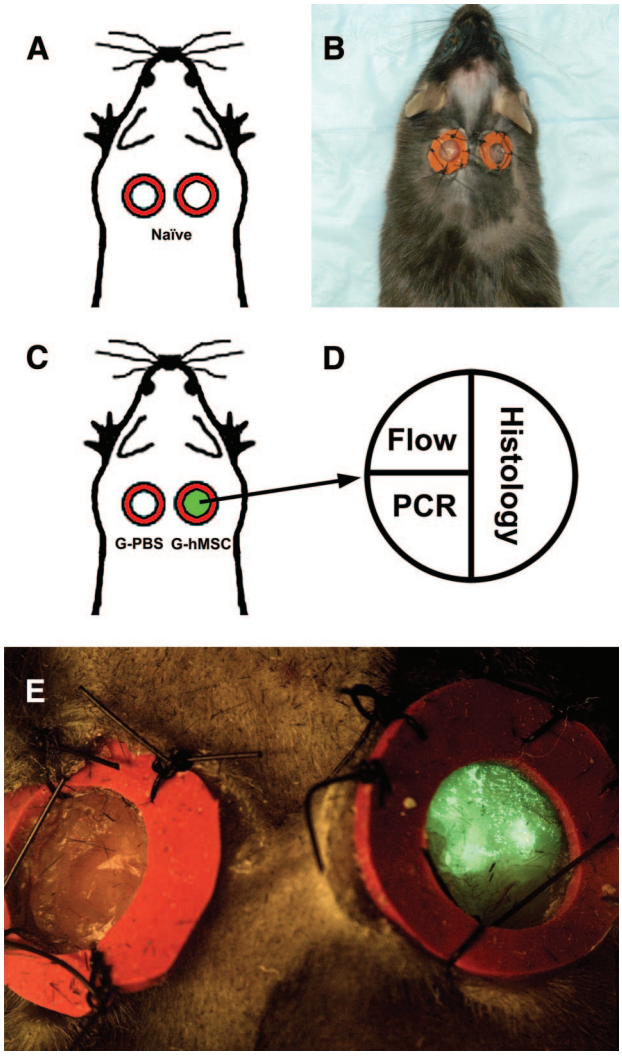

Figure 1. Schematic of the experimental design. Healthy wild-type or impaired healing diabetic mice received equal bilateral wounds in their dorsal epidermis that were held open with a splint **(A)**. Phosphate-buffered saline (PBS)-only control animals **(B)** received equivalent PBS vehicle to bilateral dorsal wounds and were never exposed to exogenous human mesenchymal stem cells (hMSCs). In experimental animals **(C)**, the left wound was treated with PBS vehicle (G-PBS group), whereas 1×10^5 green fluorescence protein (GFP)-expressing hMSC cells were delivered to the right wound (G-hMSC group). This design permitted discrimination between the direct wound healing promoting effects of local hMSCs (within the right wound) relative to their indirect effects on host response (left wound). At determined time points within the study, the wound bed was recovered and the tissue distributed as indicated **(D)** into portions for flow cytometric, gene expression, and histological analysis. The orientation of tissue division was randomized to account for variance due to unequal rates of healing across the wound bed. **(E):** The presence of GFP-expressing cells in the wound bed could be monitored in living animals by direct fluorescence stereoscopic examination ($n = 10$ per group). Abbreviations: G-hMSC, human mesenchymal stem cell-grafted; G-PBS, phosphate-buffered saline-grafted; PCR, polymerase chain reaction.

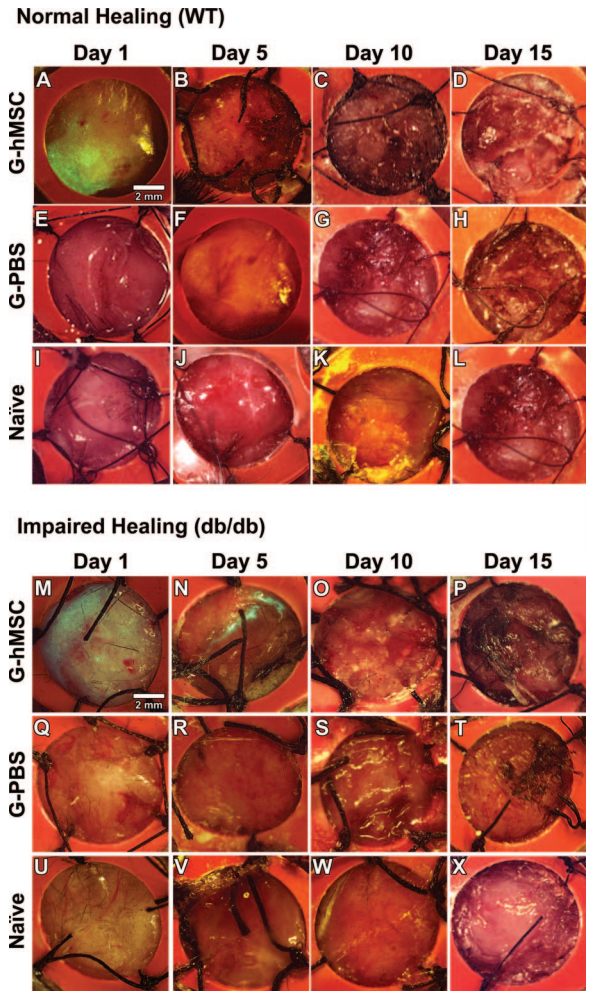

Figure 2. Green fluorescence protein (GFP)-labeled human mesenchymal stem cells (hMSCs) increased wound healing in both WT and diabetic mice. Paired standardized epidermal wounds were generated in normal healing (WT) or impaired healing (*db/db*) mice and held open by the placement of a round silicone splint sutured into place. This splint prevented contraction of the skin by dermal muscle present in rodent skin and thus mimicked the epidermal wound healing process of humans. Experimental animals ($n = 10$ per condition) received 1×10^5 hMSCs (G-hMSC) or PBS (G-PBS), and baseline controls received no engraftment to either wound (naïve/PBS). The extent of granular tissue formation and re-epithelialization was monitored daily; representative images are shown at initial treatment and at 1, 5, 10, and 15 days. GFP was visible macroscopically by stereomicroscopy during engraftment. No GFP-expressing cells were detected by macroscopic examination at 10 days postengraftment. Flow cytometric analysis confirmed the decline in detection of GFP-expressing cells over time. Yellow spots in the image are specular reflection of the light. Naïve/PBS wounds in both normal and impaired conditions healed markedly more slowly than the G-hMSC wounds and moderately more slowly than G-PBS wounds, indicating a direct and systemic response to mesenchymal stem cell engraftment. Abbreviations: G-hMSC, human mesenchymal stem cell-grafted; G-PBS, phosphate-buffered saline-grafted; WT, wild-type.

Wound Closure Is Enhanced With hMSC Delivery Despite the Disappearance of Grafted MSCs

Naïve wounds (PBS only) both in the normal and impaired healing animals exhibited significant delay in wound closure compared with their corresponding G-hMSC side (Fig. 2). Wound closure was accelerated in wound beds receiving hMSCs, and moderate improvement was noted in the G-PBS side of the same animals. Accelerated healing persisted in the G-MSC wounds through days 10 and 15, long after GFP-labeled hMSCs became undetectable (Fig. 2). We surveyed other organs, such as the lungs, liver, pancreas, and distal skin, at various end points to detect any residual hMSCs within the body and found no evidence of these cells in other locations (data not shown). We found that the G-hMSC wounds exhibited significantly improved closure in normal healing and impaired healing animals (*, $p < .05$; **, $p < .001$) at each time point, days 1, 5, 10, and 15 (Fig. 3A). Wound closure was measured using the Cavalieri point probe estimator to calculate the rate of healing (supplemental online Fig. 2). By day 15 only 54.5 $\pm$ 5.6% ($p < .05$) of the naïve/PBS normal wound area was closed, compared with the 67.3 $\pm$ 4.4% closure area seen in G-hMSC normal wounds (Fig. 3A). The G-PBS side showed significant improvement at day 10 and moderate improvement by day 15. To ensure that there was no diffusion of cells or signals and that the G-PBS side represented a systemic response, wounds were placed at varying distances within the animal, and similar closure rates were seen in distances greater than 5 mm (data not shown). Tail skin fibroblasts from WT mice were also evaluated to ensure that response to engraftment was specific to MSCs. There was no significant difference between the naïve/PBS wounds and the fibroblast engraftment in normal healing at any time point (Fig. 3A).

In impaired animals, wound beds closure was significantly improved at days 1, 5, 10, and 15 in the G-hMSC wounds. By day 15 only 28.2 $\pm$ 4.6% ($p < .001$) of the naïve/PBS *db/db* wound area was closed compared with the 56 $\pm$ 4.9% closure seen in the G-hMSC wounds (Fig. 3B). The rate of G-hMSC impaired wound healing reached baseline levels of normal healing at each time point. By day 15 there was also significantly ($p < .05$) accelerated closure on the G-PBS side as well at 41 $\pm$ 5.1%. No improvement of closure was seen with fibroblast engraftment in the impaired animals (Fig. 3B).

hMSC Engraftment Elevates Expression of Signaling Factors in the Wound Bed

The accelerated closure in the G-hMSC wounds, despite a rapid decline in the number of engrafted cells, suggest that signals within the wound bed may be systemically activated following engraftment to contribute to healing. Initial analysis of the wound bed using polymerase chain reaction (PCR) array analysis helped us determine candidate signals that were relevant to healing [17]. To discriminate between local and systemic signals, we conducted targeted RT-PCR analysis of gene expression profiles from both G-hMSC and G-PBS-treated sides of grafted animals and compared these with PBS-only naïve animals. Detection of gene expression requires the presence of the signaling cell within these locations, providing localization of the spatial distribution within the potential graft-generated niche. The timed collection of samples also provided a temporal profile of gene expression.

We found a significant (*, $p < .05$, 1.3-fold; **, $p < .001$, 2-fold) increase in the level of Wnt3a, a stem cell proliferation and transmigration factor, in the G-PBS and G-hMSC sides of the normal wounds at days 1, 5, 10, and 15 (Fig. 4A). The G-hMSC showed marked elevation compared with the G-PBS and naïve/PBS wounds as early as day 1, suggesting that Wnt3a was expressed by grafted cells. Production of Wnt3a by both human

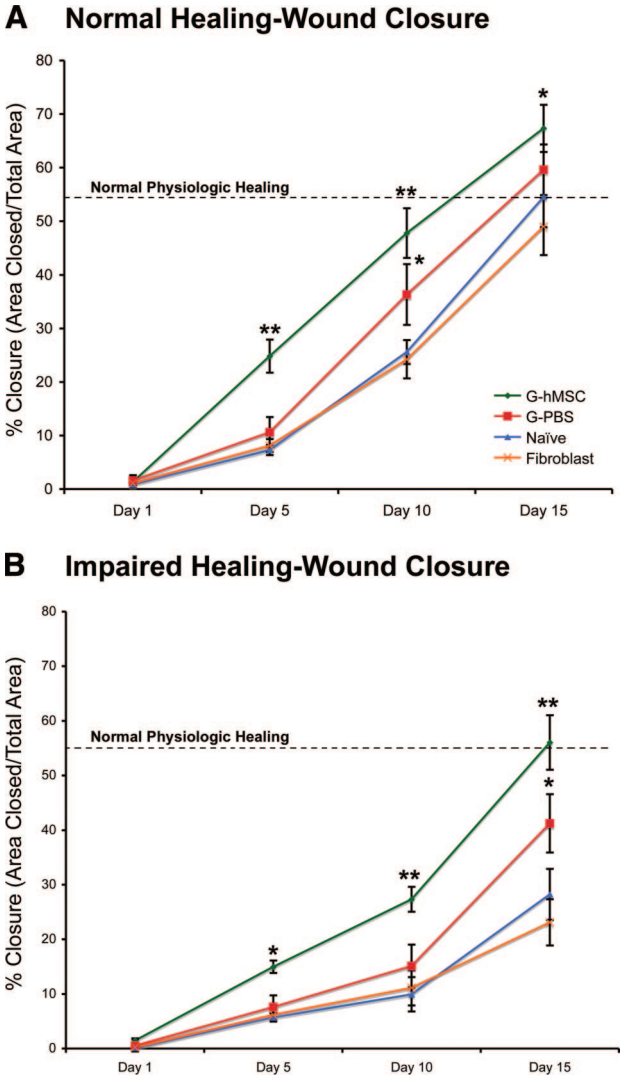

Figure 3. Grafted mesenchymal stem cells (MSCs) accelerate wound closure in wounded diabetic mice. Normal healing **(A)** and impaired healing **(B)** wounds were evaluated by treatment groups G-hMSC (green), G-PBS (red), naïve/PBS (blue), and fibroblast (orange). For both normal and impaired healing animals, naïve/PBS wounds healed significantly more slowly than the G-hMSC side at every time point. G-PBS wounds showed moderate improvement compared with the naïve/PBS wounds, whereas fibroblasts were ineffectual at improving closure. G-hMSC wounds in impaired animals were able to reach a level of healing similar to that of naïve/PBS wounds in normal healing animals. Each data point represents the mean of the percentage of the area closed. Closure was calculated from stereological analysis of micrographs using the Cavalieri point probe estimator (error bars indicate ±SEM; $n = 10–13$ per group; *, $p < .05$; **, $p < .001$; supplemental online Fig. 2). The dashed horizontal line indicates the extent of closure attained by untreated, normal healing mice at 15 days and is provided to facilitate comparisons. Abbreviations: G-hMSC, human mesenchymal stem cell-grafted; G-PBS, phosphate-buffered saline-grafted.

and mouse MSCs was confirmed by Western blot analysis (supplemental online Fig. 3). The increase in Wnt3a signal corresponded with acceleration in healing. Fibroblasts, which did not improve closure, showed no expression in Wnt3a (supplemental online Fig. 3). Elevation in expression of the angiogenic factor VEGF was seen only in the G-hMSC side at days 5 and 10 (Fig. 4B). However, PDGFRα expression was elevated earlier at day 1 and maintained at days 5 and 10 (Fig. 4C). Increased expression of PDGFRα was also noted in the G-PBS side at day 5.

In the impaired healing animal, expression of Wnt3a was highest ($p < .001$) at the earlier time points days 1 and 5 in the G-hMSC and G-PBS wounds (Fig. 4D). A significant increase of Wnt3a expression ($p < .05$) was also seen at days 10 and 15 on the G-hMSC side. Increased expression of the angiogenic factor VEGF was only seen at day 5 in the G-hMSC wounds (Fig. 4E), whereas elevation in PDGFRα expression was seen at days 1 and 5 (Fig. 4F).

Endogenous Cells Are Recruited to the Site of Injury After hMSC Engraftment

We have shown that hMSCs were not maintained in the wound bed (Fig. 2; supplemental online Fig. 1A–1J; supplemental online Fig. 4). To identify potential cellular sources of the signaling factors measured above, we assessed any potential endogenous cell populations recruited to the wound bed by using species-specific surface markers and flow cytometry to discriminate the presence of human and mouse cells. We identified host stem cells within the G-hMSC, G-PBS, and naïve/PBS wounds by using mouse-specific CD34, CD90, and CD166 (Fig. 5). These markers are representative of hematopoietic (CD34) and mesenchymal stem cells (CD90 and CD166) within the wound bed. All mouse markers were validated as having no cross-reactivity with human cells to ensure an appropriate detection of the endogenous response. Measured cell populations from G-PBS and G-hMSC sides at day 1 did not differ from the control naïve/PBS wounds (data not shown), thus representing the baseline endogenous cell populations in both normal and impaired healing animals.

Within normal healing (wild-type) animals, naïve/PBS wound beds showed an increase in endogenous MSCs at day 5, which was sustained through day 10. A limited number of non-MSCs were detected in naïve/PBS wounds. Following engraftment, there was a large influx of endogenous CD90-positive cells in both the normal healing G-hMSC and G-PBS sides at day 5. This increase was sustained in the G-hMSC side until day 10 (Fig. 5A). Similar elevations in the number of endogenous CD166 cells were also seen at days 5 and 10 in the G-hMSC and G-PBS side (Fig. 5B). In non-MSC populations, represented by CD34-positive cells, the response to engraftment was modest but detectable at days 5 and 10 in the normal healing animals (Fig. 5C).

Healing impaired animals show minimal endogenous response to injury in the control naïve/PBS wounds. Wounding itself was not sufficient to recruit endogenous cells. There was minimal recruitment of host CD34, CD90, and CD166 cells to the naïve/PBS wound bed at any time point (Fig. 5D–5F). Following engraftment of hMSCs, large elevations in the CD90 and CD166 populations were evident at days 5 and 10 (Fig. 5D, 5E). A modest increase was noted in the host CD34 population at day 5 and sustained through day 10 (Fig. 5F).

hMSC Engraftment Recruits Pre-Existing Proliferating Cells to the Wound Bed

We observed an apparent decline with GFP-expressing cells in the wound bed during healing (supplemental online Fig. 1) that coincided with an increase in endogenous stem cells within the wound by day 5 (Fig. 5). We asked whether these endogenous cells already existed or whether new cells were generated in response to wounding and engraftment by using dual thymidine analogs to discriminate between pre-existing cell populations and newly generated cells. We assessed the relative presence of

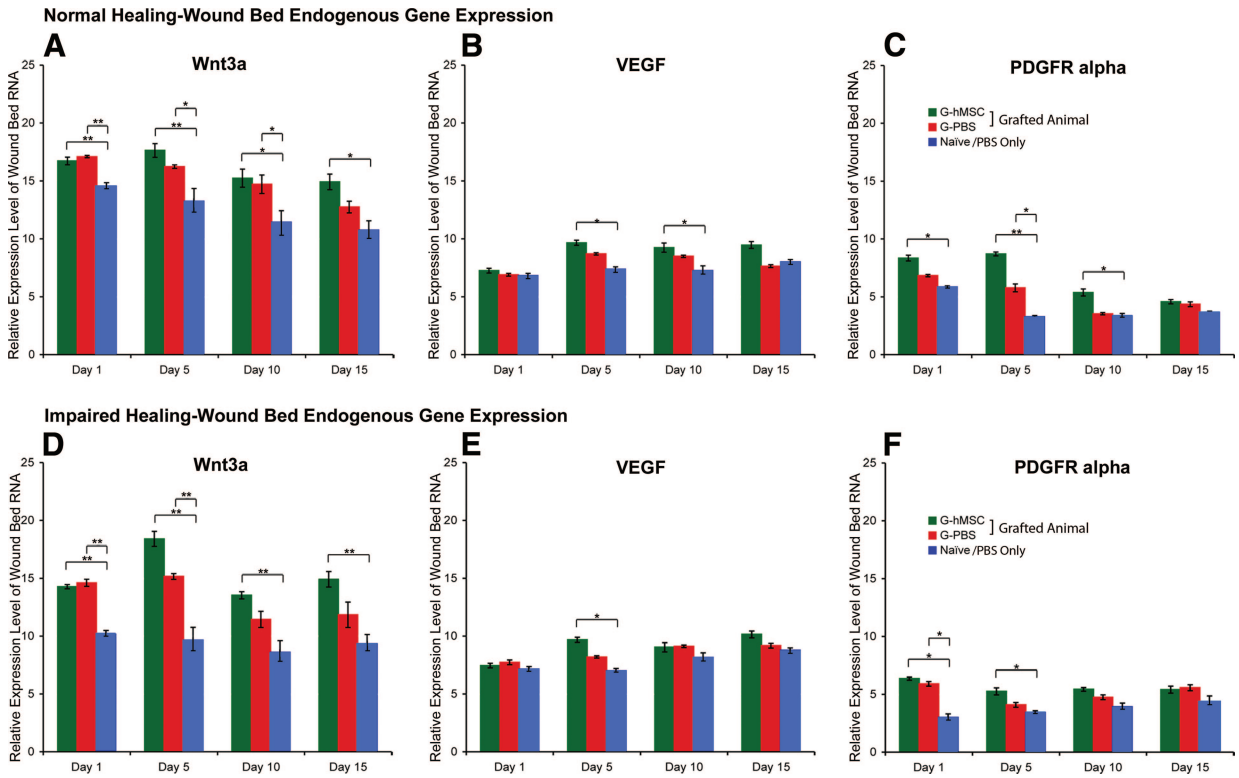

Figure 4. Reverse transcription-polymerase chain reaction analysis of wound bed endogenous gene expression. Normal healing (nondiabetic) and impaired healing (diabetic) wounds were analyzed for gene expression of Wnt3a **(A, D)**, VEGF **(B, E)**, and PDGFRα **(C, F)**. There were significant differences between grafted subjects (both G-hMSC and G-PBS conditions) and untreated subjects (naïve/PBS only) in both the normal and impaired healing animals. Whereas there was less difference in the amount of VEGF expression, there were early differences in the level of PDGFRα. Columns represent the relative expression of each factor compared with the housekeeping gene GAPDH (error bars indicate $\pm$SEM; $*$, $p < .05$; $**$, $p < .01$). Abbreviations: G-hMSC, human mesenchymal stem cell-grafted; G-PBS, phosphate-buffered saline-grafted; PBS, phosphate-buffered saline; PDGFR, platelet-derived growth factor receptor; VEGF, vascular endothelial growth factor.

these cell populations within the wound bed using IdU- and CldU-specific markers for flow cytometric analysis. The IdU-positive population identified the population of proliferating pre-existing endogenous cells recruited to the wound bed. The CldU-positive population identified the population of newly generated cells that underwent DNA synthesis following grafting or wounding. The distribution of IdU-positive and CldU-positive cells within naïve/PBS animals (Fig. 6D, 6G) defined the baseline response to wounding in the normal and impaired healing animals. The distribution of labeled cells within the G-hMSC wound beds (Fig. 6B, 6E) identified the direct recruitment response to engraftment, whereas the G-PBS cell distribution data (Fig. 6C, 6F) revealed the extent of recruitment due to the systemic response. Under all conditions (G-hMSC, G-PBS, and naïve/PBS) within normal healing animals, the recruitment of pre-existing cells in the wound bed was much greater than the number of cells proliferating in response to injury and treatment. Impaired healing animals showed similar recruitment of pre-existing endogenous cells during healing. No increase of newly generated cells was noted.

Discussion

The development of cell-mediated therapies using MSCs has been widely evaluated in a variety of injury models. Despite the increasing evidence that grafted hMSCs stimulate healing through indirect mechanisms rather than through direct participation and incorporation into tissue, the contribution of the host response has not been defined. We demonstrated that hMSC-mediated repair is largely due to the modulation and direction of host cells. The introduction of soluble factors provided by exogenous engraftment created a niche for the recruitment of endogenous MSCs and progenitor cells to the area of injury. In both the normal and impaired healing models pre-existing cells were called upon for repair. These signals were maintained following the disappearance of hMSCs from the wound. The sustained elevations of proliferative and angiogenic signals such as Wnt3a, VEGF, and PDGFRα in the grafted wounds after the loss of hMSCs indicate that the wound bed is actively participating in healing process. Here we showed that although the hMSCs are a useful tool for healing, it is the signals that they release that are critical for repair. We propose that understanding this mobilization and direction of endogenous cells will be the key to success in future therapies.

MSC delivery has been investigated in a range of clinical trials, including graft-versus-host disease, Crohn's disease, diabetes (type 1), bone defects, and cardiomyopathy [7, 24]. Systemic administration of MSCs has been reported to improve ventricular function and functional capacity and to reduce mortality in an animal model of myocardial infarction through homing and the release of paracrine angiogenic, antiapoptotic, and mitogenic factors [8, 25, 26]. As a result, the capacity of systemically delivered MSCs to exhibit specific localization to sites of injury has resulted in MSCs being

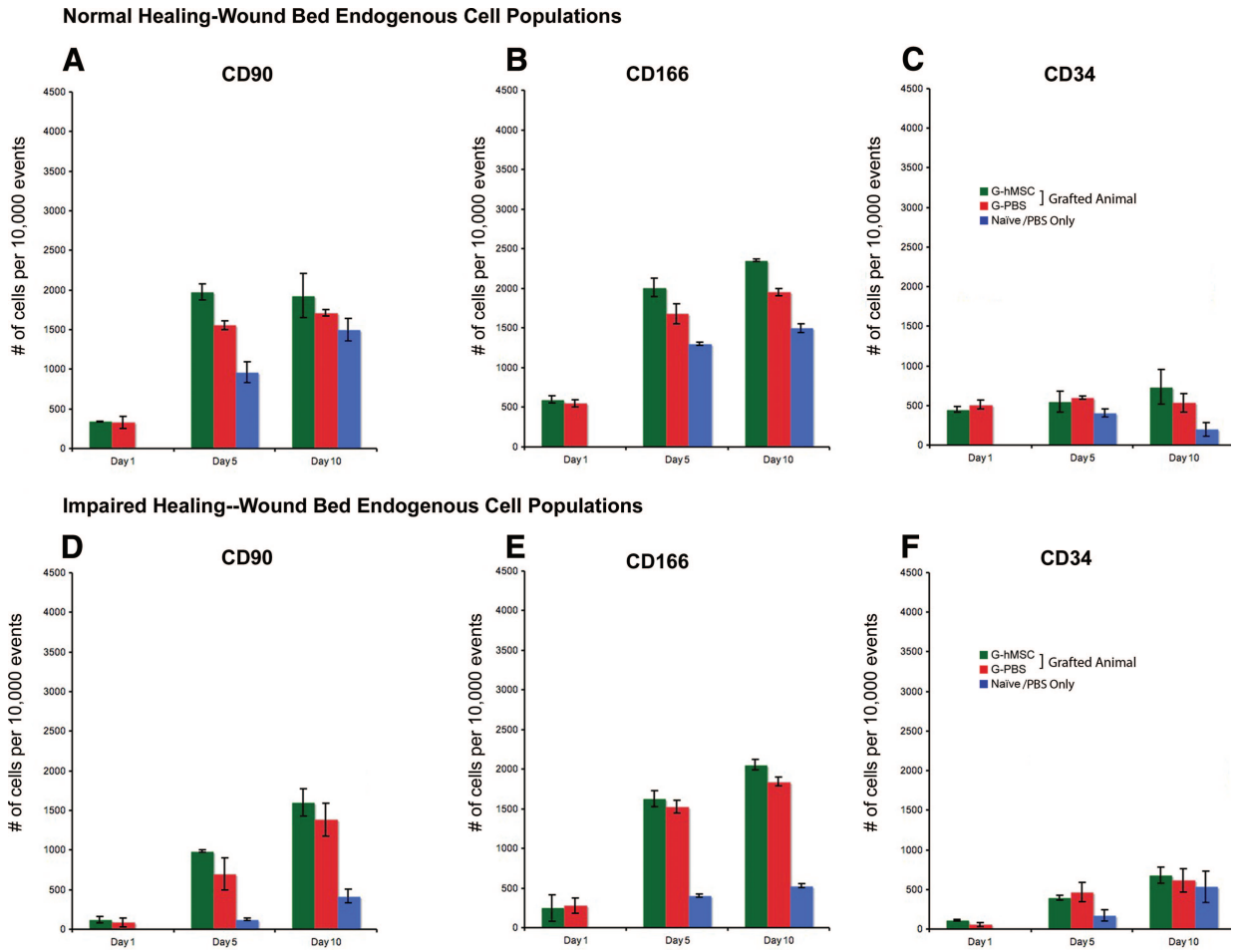

Figure 5. Grafted human mesenchymal stem cells (hMSCs) elicit recruitment of a robust endogenous stem/progenitor cell population to both grafted (G-hMSC) and nongrafted (G-PBS) wound beds. **(A–C):** Normal healing assessment of flow cytometric detection for a panel of MSC selection markers including CD34 (mouse-specific non-MSC marker-hematopoietic progenitor cell marker), CD90 (Thy1 pan-mouse MSC marker), and CD166 (mouse-specific activated leukocyte cell adhesion molecule and pan-MSC marker) reveals a mixed profile for CD34 changes relative to naïve/PBS animals (blue bars). However, CD90 and CD166 both showed substantial increase relative to the naïve/PBS, suggesting increased presence of endogenous MSCs in wound beds (G-hMSC and G-PBS) of grafted animals. Importantly, this included elevation in the G-PBS sides, indicating that grafted hMSCs may initiate a general host response. **(D–F):** Impaired healing assessment indicates a minimal response of endogenous cells in the naïve/PBS wound. Robust increases in MSC markers were noted both in the G-hMSC and G-PBS sides of grafted animals. Moderate improvement of CD34 was also noted. Each column represents total number of counted cells out of 10,000 events (error bars indicate $\pm$SEM); $n = 10$ animals per group. Abbreviations: G-hMSC, human mesenchymal stem cell-grafted; G-PBS, phosphate-buffered saline-grafted; PBS, phosphate-buffered saline.

regarded as a "magic bullet" for repair of a variety of tissues [27, 28]. Although the beneficial trial outcomes are encouraging, poor understanding of how grafted MSCs effect repair is a critical barrier to advancing the use of MSC-based treatments. Conventional cell-mediated therapies rely on targeting of exogenous MSCs to the area of injury; however, the known lack of efficiency in the homing of grafted cells and accumulating evidence that the mechanism of action may be indirect led us to investigate the participation of the endogenous environment in healing. We reasoned that grafted cells might express signals that contribute to healing by initiating recruitment of host cells such as endogenous MSCs.

It has been proposed that the capacity of MSCs to produce a variety of signals that provide molecular cues for regenerative pathways may allow endogenous MSCs to contribute to tissue repair [29–31]. MSCs reside in niches throughout the body to support other cell populations engaged in tissue maintenance and repair [32, 33]. For example, MSCs support hematopoietic cells in expansion and homing within the bone marrow [33]. MSCs have also been shown to modulate cells that contribute to healing, such as fibroblasts [34]. Furthermore, we showed here that fibroblasts alone do not promote wound healing and that they do not provide the same signaling as do MSCs when introduced to the same environment. It is known that MSCs from bone marrow release growth factors such as epidermal growth factor, fibroblast growth factor, platelet-derived growth factor (PDGF), VEGF, and stromal cell-derived factor-1, all of which can direct and regulate endogenous fibroblasts and endothelial cells [28, 34, 35]. MSCs throughout the body show significant chemotaxic response to such factors, including PDGF, VEGF, and Wnt3a, which is in agreement with our results [34, 36, 37]. The niche created by the expression of such factors attracts endogenous MSCs to the area of injury, activating the body's ability to heal and enhancing wound healing. Without engraftment, there was minimal endogenous MSC recruitment to the area of injury in the naïve/PBS impaired healing

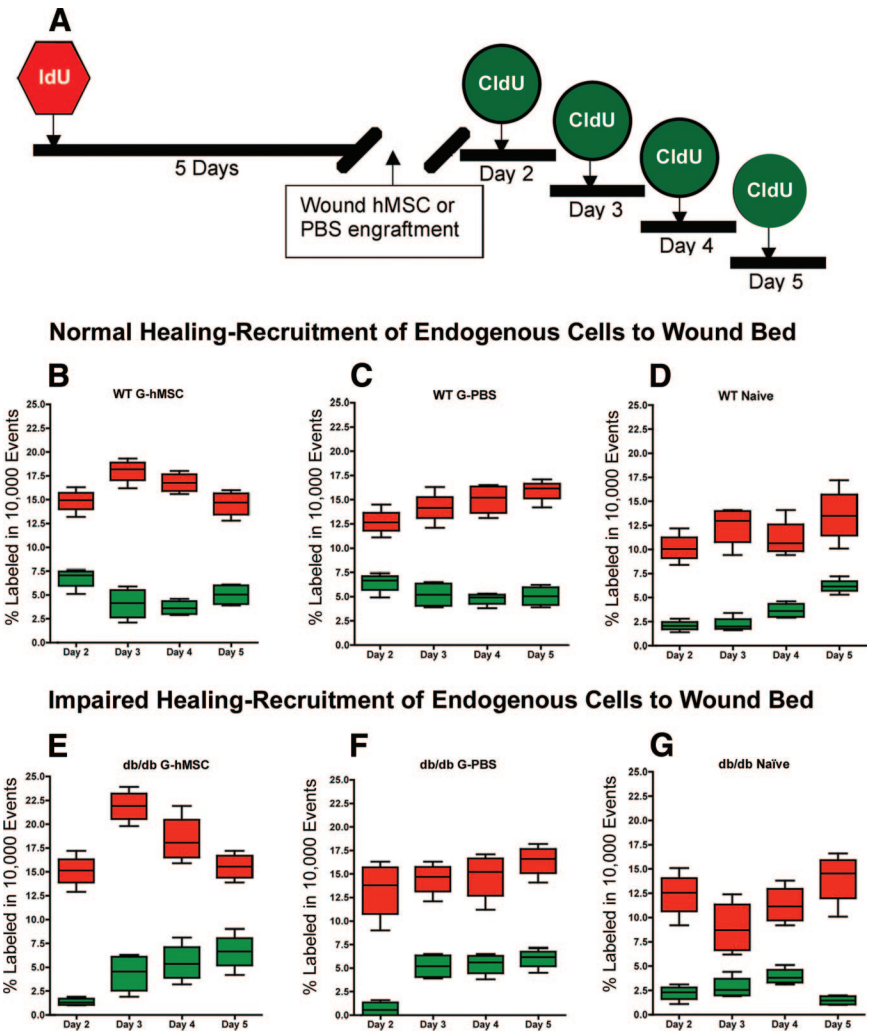

Figure 6. Cells recruited to the wound bed were generated prior to wounding and engraftment. **(A):** The experimental design of dual labeling using IdU and CldU to discriminate between two endogenous populations: those generated before wounding/grafting and those generated after wounding/grafting. Animals were pulsed with IdU 5 days before engraftment or injury to label all existing proliferating cells. To identify cells proliferating following injury and treatment, CldU was pulsed on one of four successive days after grafting. Wound bed tissue was collected 2 hours following CldU delivery at days 2, 3, 4, and 5. **(B–D):** Under all conditions within normal healing animals, the population of pre-existing cells in the wound bed (IdU; red) was greater than the number of cells proliferating in response to injury and treatment (CldU; green). In fact, the population of newly generated CldU cells was so low as to approach the limit of detection. **(E–G):** Impaired healing animals showed similar recruitment of pre-existing endogenous cells during healing. No increase in newly generated cells was noted. Box and whisker plots represent percentage of positive IdU or CldU cells out of 10,000 events (box indicates 90% confidence interval; horizontal line indicates mean; error bars represent population distribution ± SD; n = 10 animals per group, per time point). Abbreviations: CldU, chlorodeoxyuridine; G-PBS, phosphate-buffered saline-grafted; hMSC, human mesenchymal stem cell; IdU, iododeoxyuridine; PBS, phosphate-buffered saline; WT, wild-type.

animals. After engraftment, endogenous MSCs were mobilized to the wound in both the normal and impaired healing animals. Thus we propose that the signals provided by hMSCs recruited host cells and were capable of restoring healing in the impaired animal to a normal physiologic level and actually accelerated healing in healthy subjects.

Given the existence and capacity of endogenous MSCs, we asked to what extent their recruitment to a site of injury contributes to healing. In contrast to systemic delivery of MSCs to the blood circulation, we used a tightly controlled local delivery of cells to the wound bed to track grafted hMSCs in vivo during healing. This provided us with an easily accessible injury site, revealing host stem/progenitor cell homing in response to exogenous MSC signals as a key component of wound healing. By using a dual-wound design that discriminates the local response from the systemic response, we are able to identify key signals involved in the healing. The broad systemic response extends beyond the grafted side, and we see an elevation in key signals such as Wnt3a. Wnt3a has been shown to improve the migratory capacity and the proliferation potential of MSCs in vitro [38]. Importantly, this increase in Wnt3a signaling persists even after the disappearance of grafted cells, emphasizing the importance of host participation in the repair process. One proposed mechanism of MSC repair is cell-to-cell interaction between the host and the grafted cells [8, 34]. Enhanced healing exhibited by the systemic side demonstrates independence from cell-to-cell interaction. Here we show that the key to repair is not exogenous MSC targeting but rather the recruitment of host MSCs. We also show that the host cells recruited to the wound existed prior to injury. Thus, the healing response can be initiated without generating new cells, as reserves of cells exist within the body that are capable of repair once recruited.

Conclusion

These results offer new insight into the mechanism of MSC-mediated therapies. We show that significant repair initiated by grafted MSCs can continue following the absence of these engrafted cells, suggesting a major contribution to the healing wound environment by host MSCs. Thus, these findings broaden our view of therapeutic targets to include the host response. We showed that the improvement in impaired and normal wound healing has significant clinical relevance for all wounds, both chronic and acute. Future work will need to address whether the introduction of signals alone can harness the potential of these cells and is sufficient to elicit the same recruitment as MSC engraftment. This insight into the specific signals involved in recruiting endogenous stem/progenitor cells will help to advance the development of cell-free therapies that may use small molecules or drugs for repair of tissue injury, providing an alternative

to the more costly and regulatory-intensive cell-mediated therapies.

Acknowledgments

This work was funded by a Rosalind Franklin University of Medicine and Science Intramural Grant (to D.A.P.), a Department of Energy Grant (DE SC001810; to D.A.P.), and an American Diabetes Association Clinician Scientist Training Grant (7-08 CST-02; to L.S.). We thank Dr. D. Prockop for the human MSCs, Dr. R. Marr for the viral vectors, and S. Surridge for help with the figure designs.

Author Contributions

L.S.: conception and design, collection of data, data analysis and interpretation, financial support, manuscript writing; D.A.P.: financial support, conception and design, manuscript writing, final approval of manuscript.

Disclosure of Potential Conflicts of Interest

The authors indicate no potential conflicts of interest.

References

1 Sorrell JM, Caplan AI. Topical delivery of mesenchymal stem cells and their function in wounds. Stem Cell Res Ther 2010;1:30.

2 Crisan M, Yap S, Casteilla L et al. A perivascular origin for mesenchymal stem cells in multiple human organs. Cell Stem Cell 2008;3:301–313.

3 Chen FH, Tuan RS. Mesenchymal stem cells in arthritic diseases. Arthritis Res Ther 2008;10:223.

4 Chen L, Tredget EE, Wu PY et al. Paracrine factors of mesenchymal stem cells recruit macrophages and endothelial lineage cells and enhance wound healing. PLoS One 2008;3:e1886.

5 Wu Y, Chen L, Scott PG et al. Mesenchymal stem cells enhance wound healing through differentiation and angiogenesis. Stem Cells 2007; 25:2648–2659.

6 Prockop DJ, Gregory CA, Spees JL. One strategy for cell and gene therapy: Harnessing the power of adult stem cells to repair tissues. Proc Natl Acad Sci USA 2003;100(suppl 1): 11917–11923.

7 Karp JM, Leng Teo GS. Mesenchymal stem cell homing: The devil is in the details. Cell Stem Cell 2009;4:206–216.

8 Hatzistergos KE, Quevedo H, Oskouei BN et al. Bone marrow mesenchymal stem cells stimulate cardiac stem cell proliferation and differentiation. Circ Res 2010;107:913–922.

9 Javazon EH, Keswani SG, Badillo AT et al. Enhanced epithelial gap closure and increased angiogenesis in wounds of diabetic mice treated with adult murine bone marrow stromal progenitor cells. Wound Repair Regen 2007;15:350–359.

10 Daley GQ, Scadden DT. Prospects for stem cell-based therapy. Cell 2008;132:544–548.

11 Jackson WM, Nesti LJ, Tuan RS. Mesenchymal stem cell therapy for attenuation of scar formation during wound healing. Stem Cell Res Ther 2012;3:20.

12 Tasso R, Augello A, Boccardo S et al. Recruitment of a host's osteoprogenitor cells using exogenous mesenchymal stem cells seeded on porous ceramic. Tissue Eng Part A 2009;15: 2203–2212.

13 Le Blanc K, Frassoni F, Ball L et al. Mesenchymal stem cells for treatment of steroid-resistant, severe, acute graft-versus-host disease: A phase II study. Lancet 2008;371:1579–1586.

14 Giordano A, Galderisi U, Marino IR. From the laboratory bench to the patient's bedside: An update on clinical trials with mesenchymal stem cells. J Cell Physiol 2007;211:27–35.

15 Tolar J, Ishida-Yamamoto A, Riddle M et al. Amelioration of epidermolysis bullosa by transfer of wild-type bone marrow cells. Blood 2009;113:1167–1174.

16 Fiorina P, Pietramaggiori G, Scherer SS et al. The mobilization and effect of endogenous bone marrow progenitor cells in diabetic wound healing. Cell Transplant 2010;19:1369–1381.

17 Shin L, Peterson DA. Impaired therapeutic capacity of autologous stem cells in a model of type 2 diabetes. Stem Cells Translational Medicine 2012;1:125–135.

18 Badillo AT, Redden RA, Zhang L et al. Treatment of diabetic wounds with fetal murine mesenchymal stromal cells enhances wound closure. Cell Tissue Res 2007;329:301–311.

19 Arthur A, Zannettino A, Gronthos S. The therapeutic applications of multipotential mesenchymal/stromal stem cells in skeletal tissue repair. J Cell Physiol 2009;218:237–245.

20 Vega CJ, Peterson DA. Stem cell proliferative history in tissue revealed by temporal halogenated thymidine analog discrimination. Nat Methods 2005;2:167–169.

21 Galiano RD, Michaels J, Dobryansky M et al. Quantitative and reproducible murine model of excisional wound healing. Wound Repair Regen 2004;12:485–492.

22 Carlson MA, Thompson JS. Wound splinting modulates granulation tissue proliferation. Matrix Biol 2004;23:243–250.

23 Thomas RM, Hotsenpiller G, Peterson D. Acute psychosocial stress reduces cell survival in adult hippocampal neurogenesis without altering proliferation. J Neurosci 2007;27:2734–2743.

24 Prockop DJ, Kota DJ, Bazhanov N et al. Evolving paradigms for repair of tissues by adult stem/progenitor cells (MSCs). J Cell Mol Med 2010;14:2190–2199.

25 Braga LM, Rosa K, Rodrigues B et al. Systemic delivery of adult stem cells improves cardiac function in spontaneously hypertensive rats. Clin Exp Pharmacol Physiol 2008;35:113–119.

26 Ohnishi S, Ohgushi H, Kitamura S et al. Mesenchymal stem cells for the treatment of heart failure. Int J Hematol 2007;86:17–21.

27 Lee RH, Pulin AA, Seo MJ et al. Intravenous hMSCs improve myocardial infarction in mice because cells embolized in lung are activated to secrete the anti-inflammatory protein TSG-6. Cell Stem Cell 2009;5:54–63.

28 Meirelles Lda S, Fontes AM, Covas DT et al. Mechanisms involved in the therapeutic properties of mesenchymal stem cells. Cytokine Growth Factor Rev 2009;20:419–427.

29 Bonfield TL, Caplan AI. Adult mesenchymal stem cells: An innovative therapeutic for lung diseases. Discov Med 2010;9:337–345.

30 Augello A, Kurth TB, De Bari C. Mesenchymal stem cells: A perspective from in vitro cultures to in vivo migration and niches. Eur Cell Mater 2010;20:121–133.

31 Mouiseddine M, Francois S, Semont A et al. Human mesenchymal stem cells home specifically to radiation-injured tissues in a non-obese diabetes/severe combined immunodeficiency mouse model. Br J Radiol 2007;80(Spec no. 1):S49–S55.

32 Bianco P, Robey PG, Simmons PJ. Mesenchymal stem cells: Revisiting history, concepts, and assays. Cell Stem Cell 2008;2:313–319.

33 Méndez-Ferrer S, Michurina TV, Ferraro F et al. Mesenchymal and haematopoietic stem cells form a unique bone marrow niche. Nature 2010;466:829–834.

34 Shi Y, Hu G, Su J et al. Mesenchymal stem cells: A new strategy for immunosuppression and tissue repair. Cell Res 2010;20:510–518.

35 Tang J, Wang J, Yang J et al. Mesenchymal stem cells over-expressing SDF-1 promote angiogenesis and improve heart function in experimental myocardial infarction in rats. Eur J Cardiothorac Surg 2009;36:644–650.

36 Mishima Y, Lotz M. Chemotaxis of human articular chondrocytes and mesenchymal stem cells. J Orthop Res 2008;26:1407–1412.

37 Neth P, Ciccarella M, Egea V et al. Wnt signaling regulates the invasion capacity of human mesenchymal stem cells. Stem Cells 2006; 24:1892–1903.

38 Shang YC, Wang SH, Xiong F et al. Wnt3a signaling promotes proliferation, myogenic differentiation, and migration of rat bone marrow mesenchymal stem cells. Acta Pharmacol Sin 2007;28:1761–1774.

See www.StemCellsTM.com for supporting information available online.